

Fidelity susceptibility of one-dimensional models with twisted boundary conditions

Manisha Thakurathi,¹ Diptiman Sen,¹ and Amit Dutta²

¹*Center for High Energy Physics, Indian Institute of Science, Bangalore 560 012, India*

²*Department of Physics, Indian Institute of Technology, Kanpur 208 016, India*

(Received 8 October 2012; revised manuscript received 8 December 2012; published 21 December 2012)

Recently it has been shown that the fidelity of the ground state of a quantum many-body system can be used to detect its quantum critical points (QCPs). If g denotes the parameter in the Hamiltonian with respect to which the fidelity is computed, we find that for one-dimensional models with large but finite size, the fidelity susceptibility χ_F can detect a QCP provided that the correlation length exponent satisfies $\nu < 2$. We then show that χ_F can be used to locate a QCP even if $\nu \geq 2$ if we introduce boundary conditions labeled by a twist angle $N\theta$, where N is the system size. If the QCP lies at $g = 0$, we find that if N is kept constant, χ_F has a scaling form given by $\chi_F \sim \theta^{-2/\nu} f(g/\theta^{1/\nu})$ if $\theta \ll 2\pi/N$. We illustrate this both in a tight-binding model of fermions with a spatially varying chemical potential with amplitude h and period $2q$ in which $\nu = q$, and in a XY spin-1/2 chain in which $\nu = 2$. Finally we show that when q is very large, the model has two additional QCPs at $h = \pm 2$ which cannot be detected by studying the energy spectrum but are clearly detected by χ_F . The peak value and width of χ_F seem to scale as nontrivial powers of q at these QCPs. We argue that these QCPs mark a transition between extended and localized states at the Fermi energy.

DOI: [10.1103/PhysRevB.86.245424](https://doi.org/10.1103/PhysRevB.86.245424)

PACS number(s): 64.70.Tg, 03.67.-a, 75.10.Jm

I. INTRODUCTION

Quantum phase transitions have been studied extensively for several years. These are transitions which occur in the ground state of a many-body quantum system as a parameter g in the Hamiltonian is varied across a critical value;^{1–5} the ground state typically has different orders on the two sides of the critical point. Several measures arising in quantum information theory, such as entanglement,^{6–8} entanglement entropy,^{9,10} Loschmidt echo,¹¹ decoherence,¹² and quantum discord^{13–17} have been used to detect the location of a quantum critical point (QCP). A number of reviews have appeared on the connections between quantum critical systems and quantum information theory.^{18–21}

The concept of quantum fidelity (F) has proved to be particularly useful for detecting the locations of QCPs.^{22–37} We consider a one-dimensional system whose Hamiltonian $H(g)$ contains a parameter g such that the system is at a QCP when $g = 0$. Note that a QCP exists only in the thermodynamic limit in which the number of sites $N \rightarrow \infty$. Consider now a system in which N is finite but large ($\gg 1$). Given two ground-state wave functions $|\psi_0(g + dg/2)\rangle$ and $|\psi_0(g - dg/2)\rangle$ at two values of the parameter which are separated by a small amount dg (we assume that the ground states are nondegenerate), we define the fidelity as

$$F(g, dg) = |\langle \psi_0(g + dg/2) | \psi_0(g - dg/2) \rangle|. \quad (1)$$

First-order perturbation theory shows that in the limit $dg \rightarrow 0$, $F - 1 \rightarrow 0$ as $(dg)^2$. We therefore define the fidelity susceptibility (FS) as

$$\chi_F(g) = \lim_{dg \rightarrow 0} \frac{\ln F(g, dg)}{(dg)^2}. \quad (2)$$

(Note that our definition of the FS differs by a factor of 2 from the one given in many other papers.^{33,34}) The FS measures how rapidly the ground state changes with g . It turns out that near the QCP at $g = 0$, χ_F shows a large peak even for finite values of N because there are a large number of very low energy states

which mix with each other in a way which changes rapidly with g . Thus the FS is able to detect the ground-state singularities associated with a quantum phase transition without making explicit reference to an order parameter. In the limit $g \rightarrow 0$, it is found that^{24,31–33}

$$\chi_F(g) \sim -N|g|^{\nu-2}, \quad (3)$$

where ν is the correlation length exponent at the QCP (namely, for $N \rightarrow \infty$, the correlation length ξ diverges as $|g|^{-\nu}$ as $g \rightarrow 0$). Equation (3) holds only if $\nu < 2$; the divergence in that expression for small g arises from contributions from the low-energy (critical) modes. However, if $\nu \geq 2$, Eq. (3) is no longer useful for finding QCPs because, for small g , the contributions to χ_F from high-energy modes are of the same order as (if $\nu = 2$) or dominate over (if $\nu > 2$) the terms of order $|g|^{\nu-2}$.

We will show in this paper that even if $\nu \geq 2$, we can use χ_F to locate a QCP by using twisted boundary conditions labeled by a twist angle $N\theta$ and taking the limit $\theta \rightarrow 0$ in a particular way. The introduction of θ allows us to bring the energy of one particular state arbitrarily close to zero; this state then contributes a term to χ_F which scales with θ as $\theta^{-2/\nu} f(g/\theta^{1/\nu})$. In the limit of $\theta \rightarrow 0$, a plot of χ_F versus g clearly shows the divergence due to $\theta^{-2/\nu}$ at $g \sim \theta^{1/\nu}$, thereby pinpointing the location of the QCP.

The paper is organized as follows. In Sec. II A, we will present a simple argument to show that the presence of a twist angle $N\theta$, along with a gap proportional to g^ν , gives rise to a χ_F which exhibits the above scaling form. In Sec. II B, we indicate how this result may be generalized to higher dimensions. In Secs. III A–III C, we will illustrate how this works in a tight-binding model of noninteracting spinless fermions with a periodic chemical potential with amplitude h and period $2q$, where q is an integer. This model has a QCP at $h = 0$ where $\nu = q$; it therefore allows us to study the scaling of χ_F for different values of ν . In Sec. III D, we will illustrate the scaling of χ_F with θ in a spin-1/2 chain which has a QCP with

$\nu = 2$. In Sec. IV, we will consider the case of large values of q and numerically show that χ_F has a scaling form near $h = \pm 2$ with nontrivial power laws. (This study is motivated by the observation that the Aubry-Andre model, which has a quasiperiodic chemical potential, has transition from extended to localized wave functions at $h = \pm 2$.) In Sec. V, we will summarize the results presented in this paper.

II. FIDELITY SUSCEPTIBILITY FOR A TWO-STATE SYSTEM

In this section we will do a simple calculation to determine the fidelity of a two-state system. The results obtained here will be used in the following sections.

A. One-dimensional systems

Consider a two-state problem which is governed by a Hamiltonian of the form

$$H = \begin{pmatrix} -uk & ag^\nu \\ ag^\nu & uk \end{pmatrix}. \quad (4)$$

This form is motivated as follows. In later sections we will consider a one-dimensional model in which $\pm k$ will denote the momenta of two states close to zero energy (measured with respect to the Fermi energy), u will denote the Fermi velocity obtained by linearizing the dispersion near zero energy, g will denote a parameter in a many-body Hamiltonian such that the QCP lies at $g = 0$, and a is some constant. The form in Eq. (4) will be taken to be valid only for values of k much smaller than some cutoff, i.e., only for low-energy modes. Since the eigenvalues of H in Eq. (4) are equal to $\pm\sqrt{u^2k^2 + a^2g^{2\nu}}$, we see that the excitation spectrum is given by $E = \pm uk$ at the QCP (which would be consistent with the dynamical critical exponent of a many-body system being given by $z = 1$), while $E = g^\nu$ for $k = 0$ is consistent, for $z = 1$, with the definition of the correlation length exponent ν .

After finding the ground state $|\psi_0(g)\rangle$ of H in Eq. (4), we can compute the FS using Eqs. (1) and (2); we find

$$\chi_F(g, k) = -\frac{\nu^2}{8g^2} \frac{1}{[ag^\nu/(uk) + uk/(ag^\nu)]^2}. \quad (5)$$

In the limit $k \rightarrow 0$, we see that the FS has the scaling form

$$\chi_F(g, k) = (uk/a)^{-2/\nu} f(a^{1/\nu}g/(uk)^{1/\nu}),$$

$$\text{where } f(x) = -\frac{\nu^2}{8x^2} \frac{1}{(x^\nu + 1/x^\nu)^2}. \quad (6)$$

We note that $f(x)$ has a single peak at $x = 0$ if $\nu = 1$. If $\nu > 1$, $f(x)$ has two peaks at $x = \pm[(\nu - 1)/(\nu + 1)]^{1/(2\nu)}$, and goes to 0 as $-(\nu^2/8)x^{2(\nu-1)}$ for $x \rightarrow 0$ and as $-\nu^2/(8x^{2(\nu+1)})$ for $x \rightarrow \infty$.

Next, let us suppose that we are considering a many-body system with size N , so that the momenta are quantized as $k = \theta + 2\pi n/N$, where n runs over all integers, and θ comes from a twisted boundary condition to be elaborated in later sections. The presence of the $2\pi n/N$ term implies that we can take θ to lie in the range $[0, 2\pi/N]$. If the Hamiltonian of the system can be decomposed into independent two-state

systems of the form given in Eq. (4), the FS will be given by

$$\chi_F(g) = -\frac{\nu^2}{8g^2} \sum_{n=-\infty}^{\infty} \frac{1}{\left(\frac{ag^\nu}{u(\theta+2\pi n/N)} + \frac{u(\theta+2\pi n/N)}{ag^\nu}\right)^2}. \quad (7)$$

We can now consider the value of χ_F in various limits.

First, if N is held fixed and we consider a regime in which $ag^\nu, u\theta \ll 2\pi u/N$ and $a^{1/\nu}g/(u\theta)^{1/\nu}$ is of order 1, the sum in Eq. (7) will be dominated by the $n = 0$ term and we will obtain the scaling form

$$\chi_F(g) = (u\theta/a)^{-2/\nu} f(a^{1/\nu}g/(u\theta)^{1/\nu}), \quad (8)$$

where the function f is given in Eq. (6). Second, if $g^\nu \ll 2\pi u/N$ but θ is of order $2\pi/N$, then we obtain

$$\chi_F(g) = -\frac{\nu^2 a^2 g^{2(\nu-1)}}{8u^2} \sum_{n=-\infty}^{\infty} \frac{1}{(\theta + 2\pi n/N)^2}$$

$$= -\frac{N^2 a^2 \nu^2 g^{2(\nu-1)}}{32u^2 \sin^2(N\theta/2)}. \quad (9)$$

As $g \rightarrow 0$, Eq. (9) shows that χ_F has a finite limit if $\nu = 1$ but it goes to 0 if $\nu > 1$. [For the models that we will consider later, Eq. (4) is *not* a good approximation for $|k| \gg g^\nu$ (high-energy modes), and the contributions to the FS from such modes generally approaches a nonzero value as $g \rightarrow 0$ as we will show in Eq. (33) for $\nu > 1$.] Finally, if $2\pi/N \ll g^\nu$, the sum in Eq. (7) can be replaced by an integral over $k = 2\pi n/N$; if we further assume that $g^\nu \ll 1$, the limits of the integral can be taken to be $\pm\infty$ since the contributions from the regions with $|k| \gg g^\nu$ will be negligible. We then obtain

$$\chi_F(g) = -\frac{N\nu^2}{8g^2} \int_{-\infty}^{\infty} \frac{dk}{2\pi} \frac{1}{[ag^\nu/(uk) + uk/(ag^\nu)]^2}$$

$$= -\frac{N\nu^2 ag^{\nu-2}}{32u}. \quad (10)$$

[The integral in the above equation only gets substantial contributions from values of $|k|$ lying around g^ν , i.e., from low-energy modes. The scaling given in Eq. (10) will therefore be valid as long as Eq. (4) is a good approximation for such low-energy modes, even if it fails for high-energy modes.] We thus see from Eq. (10) that as $g \rightarrow 0$, the FS will diverge if $\nu < 2$ but not if $\nu \geq 2$. A plot of the FS versus g will therefore show a divergence at the QCP ($g = 0$) only if $\nu < 2$, but for $\nu \geq 2$, the FS will not be useful for finding the location of the QCP.

We conclude that for a large but finite value of the system size N , the FS can detect a QCP only if $\nu < 2$. Note that this conclusion would not change if we replaced k and g^ν by k^z and $g^{z\nu}$, respectively, in Eq. (4), with a dynamical critical exponent z which is not equal to 1. The exponent which appears in the second line in Eq. (10) will be $\nu - 2$ regardless of the value of z .

B. Higher dimensional systems

Although the rest of this paper will be only concerned with one-dimensional systems, let us briefly discuss what may happen in higher dimensions. We assume that there is a d -dimensional system in which the modes with momenta $\pm\vec{k}$ are governed by a Hamiltonian of the form given in Eq. (4),

where the momentum variable in that equation now stands for $k = |\vec{k}|$. Equations (5) and (6) will continue to hold. Next, let us impose periodic boundary conditions, with a twist angle θ in one of the d dimensions and zero twist angle in the remaining $d - 1$ dimensions. To be specific, we assume that we have a hypercubic lattice system which has N sites in each dimension, so that the different momenta are quantized as $k_i = 2\pi n_i/N$; the twist shifts the first momentum to $k_1 = \theta + 2\pi n_1/N$. Equation (7) then gets modified to

$$\chi_F(g) = -\frac{v^2}{8g^2} \sum_{n_1, \dots, n_d = -\infty}^{\infty} \frac{1}{\left(\frac{ag^v}{uk'} + \frac{uk'}{ag^v}\right)^2}, \quad (11)$$

$$k' = \left[(\theta + 2\pi n_1/N)^2 + \sum_{i=2}^d (2\pi n_i/N)^2 \right]^{1/2}.$$

As before, we can now consider what happens in three different cases.

If N is held fixed, $ag^v, u\theta \ll 2\pi u/N$ and $g/(u\theta)^{1/v}$ is of order 1, the sum in Eq. (11) will be dominated by the term in which $n_i = 0$ for all i . Then we will obtain the scaling form given in Eq. (8) where the function f is given in Eq. (6). Note that the scaling form does not depend on the dimensionality d in this case. Next, if $g^v \ll 2\pi u/N$ but θ is of order $2\pi/N$, then we obtain

$$\chi_F(g) = -\frac{N^2 v^2 a^2 g^{2(v-1)}}{8u^2} \times \sum_{n_1, \dots, n_d = -\infty}^{\infty} \frac{1}{(N\theta + 2\pi n_1)^2 + \sum_{i=2}^d (2\pi n_i)^2}. \quad (12)$$

As $g \rightarrow 0$, Eq. (12) has a finite limit (which depends on $N\theta$) if $v = 1$ but goes to 0 if $v > 1$. Finally, if $2\pi/N \ll g^v$, the sum in Eq. (11) can be replaced by an integral over $k_i = 2\pi n_i/N$; assuming that $g^v \ll 1$, the limits of the integral can be taken to be $\pm\infty$. We then obtain

$$\chi_F(g) = -\frac{N^d v^2}{8g^2} \int_{-\infty}^{\infty} \frac{d^d k}{(2\pi)^d} \frac{1}{[ag^v/(u|\vec{k}|) + u|\vec{k}|/(ag^v)]^2} \sim -N^d a^d g^{dv-2}. \quad (13)$$

(A similar scaling relation was found by adiabatic perturbation theory.^{32,33}) As $g \rightarrow 0$, Eq. (13) diverges if $dv < 2$ but not if $dv \geq 2$. A plot of χ_F therefore diverges at the QCP if $dv < 2$, but for $dv \geq 2$, χ_F is not useful for locating the QCP.

III. TIGHT-BINDING MODEL WITH VARIABLE v

We will now study fidelity in a one-dimensional tight-binding model of spinless fermions in which the exponent v can take any integer value; this will illustrate many of the points discussed in Sec. II. In Sec. III A, we will discuss the model and its energy spectrum close to zero energy, while in Sec. III B, we will examine a number of features related to fidelity.

A. The model

The model that we are interested in was studied recently from the point of view of quenching dynamics across a QCP.^{38,39} In this section, we will summarize the relevant

discussion from Ref. 38. The Hamiltonian is given by

$$H = -\sum_{n=1}^N \left[J(e^{i\theta} c_n^\dagger c_{n+1} + e^{-i\theta} c_{n+1}^\dagger c_n) + h \cos\left(\frac{\pi n}{q} + \phi\right) c_n^\dagger c_n \right], \quad (14)$$

where q is a positive integer, N is the system size, and we have imposed periodic boundary conditions so that $c_{N+1} \equiv c_1$. (We will set the hopping amplitude J , \hbar and the lattice spacing a equal to unity.) Note that one can perform a unitary transformation on the c_n , namely, $c_n \rightarrow e^{-in\theta} c_n$, which removes the phase θ from all the hopping terms except for the hopping between the sites at N and 1 where the phase becomes $e^{\pm iN\theta}$; this is called a twisted boundary condition, with $N\theta$ being the twist angle. We can assume that $0 \leq N\theta \leq 2\pi$, namely, that θ lies in the range $[0, 2\pi/N]$. The usual periodic boundary condition corresponds to $\theta = 0$. The period of the chemical potential in Eq. (14) is $2q$, and we will assume that N is a multiple of $2q$. A chemical potential of this form appears in the Azbel-Hofstadter model.⁴⁰⁻⁵¹ Since shifting $n \rightarrow n + 1$ in Eq. (14) is equivalent to shifting $\phi \rightarrow \phi + \pi/q$, we can assume without loss of generality that ϕ lies in the range $[0, \pi/q]$.

The fermionic operators can be Fourier transformed to the momentum basis,

$$c_k = \frac{1}{\sqrt{N}} \sum_{n=1}^N c_n e^{-ikn}, \quad (15)$$

where the momentum k goes from $-\pi$ to π in units of $2\pi/N$; these operators satisfy the anticommutation rules $\{c_k, c_{k'}^\dagger\} = \delta_{k,k'}$. In momentum space, the first two terms of the Hamiltonian in Eq. (14) have the tight-binding form

$$H_0 = -\sum_{k=-\pi}^{\pi} 2 \cos(k + \theta) c_k^\dagger c_k. \quad (16)$$

For the last term in Eq. (14), we use the decomposition

$$h \cos\left(\frac{\pi n}{q} + \phi\right) = \frac{h}{2} (e^{i(\pi n/q + \phi)} + e^{-i(\pi n/q + \phi)}). \quad (17)$$

Hence this term couples two fermionic modes with momenta k_1 and k_2 if $k_1 = k_2 \pm \pi/q$. This fragments the total Hamiltonian H into $N/(2q)$ decoupled Hamiltonians H_k which are labeled by a momentum k lying in the range $-\pi$ to $-\pi + \pi/q$; namely,

$$H = \sum_{k=-\pi}^{-\pi + \pi/q} H_k. \quad (18)$$

For each k , H_k can be written as a $(2q)$ -dimensional matrix involving the momenta $k + r\pi/q$, where $r = 1, 2, \dots, 2q$. The matrix elements of H_k are given by

$$\begin{aligned} \langle k + r\pi/q | H_k | k + s\pi/q \rangle \\ = -2 \cos(k + \theta + s\pi/q) \delta_{r,s} \\ - (h/2) (e^{i\phi} \delta_{r,s+1} + e^{-i\phi} \delta_{r,s-1}), \end{aligned} \quad (19)$$

where $1 \leq r, s \leq 2q$, and we have set $J = 1$. In writing Eq. (19), we have assumed ‘‘periodic boundary conditions’’ for the matrix H_k , so that $r = 0$ and $2q + 1$ mean $r = 2q$ and 1, respectively.

Before proceeding further, let us point out an interesting consequence of the decoupling of H into a sum of H_k and then a duality symmetry.^{42,45} Suppose that the system has a parameter θ and $N = 2qr$ sites, where r is a positive integer. Since the momentum k is quantized in units of $2\pi/N$, and only momenta differing by integer multiples of π/q are coupled to each other, the form of H_k in Eq. (19) implies that this system is exactly equivalent to a sum of r different systems, which have $N' = 2q$ sites each but have r different values of θ' given by $\theta, \theta + 2\pi/(2qr), \theta + 4\pi/(2qr), \dots, \theta + 2(r-1)\pi/(2qr)$. Therefore, instead of studying a system with $2qr$ sites and one particular value of θ , we can study a system with only $2q$ sites but several values of θ . Next, we observe that if $N = 2q$, the Hamiltonians in real and momentum space, Eqs. (14) and (19), get mapped into each other if we simultaneously interchange $J \leftrightarrow h/2$ and $\theta \leftrightarrow \phi$; here we have used the fact that a shift in ϕ or θ by $\pi/q = 2\pi/N$ has no effect on the spectrum. In particular, the model in Eq. (14) is self-dual if $J = h/2$ and $\theta = \phi$.

For each of the Hamiltonians H_k in Eq. (19), the $2q$ energy levels come in q pairs $\pm E$. This can be shown by shifting $s \rightarrow s + q$ which flips the sign of the first term in Eq. (19), and changing the sign of the state corresponding to s by $(-1)^s$ which flips the sign of the terms proportional to h in that equation. Assuming that there are no states at exactly zero energy, we see that the ground state of each H_k is one in which the q negative energy states are filled and the q positive energy states are empty; thus the ground state is half-filled for each H_k .

It will soon become clear that the model defined above has a QCP at $h = 0$. We therefore use perturbation theory to study the region near $h = 0$.³⁸ [We will set $\theta = 0$ in Eqs. (20)–(23); this is a reasonable approximation if N is large since we always take $0 \leq \theta \leq 2\pi/N$.] We will be particularly interested in states near zero energy which will contribute the most to the FS. Since the system is at half filling, these states lie near the momenta $k = \pm k_F$, where the Fermi momentum $k_F = \pi/2$. If the amplitude h of the chemical potential is zero, the system is gapless and the states at $k = \pm\pi/2$ are degenerate with each other. Assuming that h is small compared to the bandwidth of $4J$, we can use a perturbative expansion in h to calculate the breaking of this degeneracy. The regions near $k = -\pi/2$ and $k = \pi/2$ regions are coupled through one series of intermediate states lying at $k = -\pi/2 + \pi/q, -\pi/2 + 2\pi/q, \dots, \pi/2 - \pi/q$ (with an amplitude equal to $-he^{i\phi}$ at each step), and through another series of intermediate states lying at $k = -\pi/2 - \pi/q, -\pi/2 - 2\pi/q, \dots, \pi/2 + \pi/q$ (with an amplitude equal to $-he^{-i\phi}$ at each step). Each of these series consists of $q-1$ intermediate states. At the q th order in perturbation theory, we therefore obtain an effective Hamiltonian H_{eff} which has a matrix element between the states at $k = \pm\pi/2$ given by

$$\begin{aligned} \Delta &\equiv \langle \pi/2 | H_{\text{eff}} | -\pi/2 \rangle = \langle -\pi/2 | H_{\text{eff}} | \pi/2 \rangle^* \\ &= \frac{(-h/2)^q e^{iq\phi}}{\prod_{s=1}^{q-1} [2 \cos(-\pi/2 + s\pi/q)]} \\ &\quad + \frac{(-h/2)^q e^{-iq\phi}}{\prod_{s=1}^{q-1} [2 \cos(-\pi/2 - s\pi/q)]}, \end{aligned} \quad (20)$$

where the denominators come from factors like $E_{-\pi/2} - E_{-\pi/2 \pm s\pi/q} = 2 \cos(-\pi/2 + \pm s\pi/q)$ corresponding to the energies in the unperturbed Hamiltonian in Eq. (16). Simplifying Eq. (20) gives

$$\Delta = (-1)^q (h/2)^q \frac{e^{iq\phi} + (-1)^{q-1} e^{-iq\phi}}{\prod_{s=1}^{q-1} [2 \sin(\pi s/q)]}. \quad (21)$$

Hence the magnitude of Δ is given by

$$\begin{aligned} |\Delta| &= \frac{h^q}{4^{q-1}} \frac{|\cos(q\phi)|}{\prod_{s=1}^{q-1} \sin(\pi s/q)} \quad \text{if } q \text{ is odd,} \\ &= \frac{h^q}{4^{q-1}} \frac{|\sin(q\phi)|}{\prod_{s=1}^{q-1} \sin(\pi s/q)} \quad \text{if } q \text{ is even.} \end{aligned} \quad (22)$$

We see that ϕ governs the relative phase between the two sets of intermediate states which connect the states at $k = \pm\pi/2$. We will assume that ϕ is such that $\cos(q\phi) \neq 0$ if q is odd, and $\sin(q\phi) \neq 0$ if q is even; if these conditions are violated, we would have to go to higher order perturbation theory to find a nonzero matrix element connecting the states at $k = \pm\pi/2$.

We can now consider moving slightly away from $k = \pm\pi/2$; then the unperturbed energies of the states $k = -\pi/2 + k'$ and $\pi/2 + k'$ are given by $-2k'$ and $2k'$, respectively. The effective Hamiltonian describing these two states is then given by the 2×2 matrix

$$H_{\text{eff},k'} = \begin{pmatrix} -2k' & \Delta^* \\ \Delta & 2k' \end{pmatrix}, \quad (23)$$

where we assume that Δ continues to be given by the expression in Eq. (21) because k' is small. The eigenvalues of (23) are given by $\pm \sqrt{4k'^2 + |\Delta|^2}$; this is the dispersion of a massive relativistic particle whose velocity is equal to the Fermi velocity $u = 2$ and mass is proportional to $|\Delta| \sim h^q$ times $\cos(q\phi)$ or $\sin(q\phi)$.

Hence, $h = 0$ corresponds to a QCP where the mass gap vanishes. Given that the energy vanishes as $|k'|$ if $h = 0$ and h^q if $k' = 0$, the dynamical critical exponent and correlation length exponent are given by $z = 1$ and $\nu = q$, respectively. The correlation length exponent ν thus depends in a simple way on the periodicity of the chemical potential.

Comparing Eq. (4) with Eqs. (22) and (23), we identify $g = h$, $u = 2$, and the constant a is given by

$$\begin{aligned} a &= \frac{1}{4^{q-1}} \frac{|\cos(q\phi)|}{\prod_{s=1}^{q-1} \sin(\pi s/q)} \quad \text{if } q \text{ is odd,} \\ &= \frac{1}{4^{q-1}} \frac{|\sin(q\phi)|}{\prod_{s=1}^{q-1} \sin(\pi s/q)} \quad \text{if } q \text{ is even.} \end{aligned} \quad (24)$$

To summarize, we began with a model whose Hamiltonian in momentum space consists of a sum of $(2q)$ -dimensional Hamiltonians. Close to the QCP which lies at $h = 0$, we used perturbation theory to write an effective two-state Hamiltonian which governs pairs of low-energy states, i.e., states close to the Fermi energy. In the next section, we will use the results obtained in Sec. II A for the FS of two-state systems to obtain the FS of our model.

B. Fidelity susceptibility for various ν

We begin this section by describing how the FS can be numerically calculated for the model presented in Sec. III A. As we have seen, the Hamiltonian decouples into $N/(2q)$ Hamiltonians H_k . If we can compute the fidelity $F_k(h, dh) = |\langle \psi_{0,k}(h + dh) | \psi_{0,k}(h) \rangle|$ for each of the H_k , the total fidelity of the system will be given by the product

$$F(h, dh) = \bigotimes_{k=-\pi}^{-\pi+\pi/q} F_k(h, dh). \quad (25)$$

Next, we know that the ground state is half filled for each of the H_k for every value of h . Let $\psi_{i,k}(h)$ denote the first quantized wave functions of the filled states i ($i = 1, 2, \dots, q$); each of the $\psi_{i,k}(h)$ denotes a $(2q)$ -dimensional column which is the space on which H_k acts. Let $\psi_{i,r,k}(h)$ denote the r th component of $\psi_{i,k}(h)$ ($r = 1, 2, \dots, 2q$), and $c_{r,k}^\dagger$ denote the second quantized creation operator for the fermion corresponding to the r th component. Then the i th filled state can be written in second quantized form as $\hat{\psi}_{i,k}^\dagger(h)|\text{vac}\rangle$, where

$$\begin{aligned} \hat{\psi}_{i,k}^\dagger(h) &= \sum_{r=1}^{2q} \psi_{i,r,k}(h) c_{r,k}^\dagger, \\ \hat{\psi}_{i,k}(h) &= \sum_{r=1}^{2q} \psi_{i,r,k}^*(h) c_{r,k}, \end{aligned} \quad (26)$$

and $|\text{vac}\rangle$ denotes the vacuum state of the fermions: $c_{r,k}|\text{vac}\rangle = 0$ for all r and k . The half-filled ground state is therefore given by the second quantized expression

$$\bigotimes_{i=1}^q \hat{\psi}_{i,k}^\dagger(h)|\text{vac}\rangle. \quad (27)$$

We can now use Wick's theorem⁵² to show that

$$\begin{aligned} F_k(h, dh) &= \left| \langle \text{vac} | \bigotimes_{i=1}^q \hat{\psi}_{i,k}(h + dh/2) \right. \\ &\quad \left. \bigotimes_{j=1}^q \hat{\psi}_{j,k}^\dagger(h - dh/2) | \text{vac} \rangle \right| \end{aligned} \quad (28)$$

is given by the magnitude of the determinant of a q -dimensional matrix $M_k(h, dh)$,

$$\begin{aligned} F_k(h, dh) &= |\det[M_k(h, dh)]|, \\ (M_k(h, dh))_{ij} &= \langle \text{vac} | \hat{\psi}_{i,k}(h + dh/2) \hat{\psi}_{j,k}^\dagger(h - dh/2) | \text{vac} \rangle \\ &= \sum_{r=1}^{2q} \psi_{i,r,k}^*(h + dh/2) \psi_{j,r,k}(h - dh/2). \end{aligned} \quad (29)$$

Thus the computation of the total fidelity F reduces to finding the determinants of the matrices M_k and then multiplying the determinants over $N/(2q)$ values of k . The FS is then found as

$$\chi_F(h) = \lim_{dh \rightarrow 0} \frac{\ln F(h, dh)}{(dh)^2}. \quad (30)$$

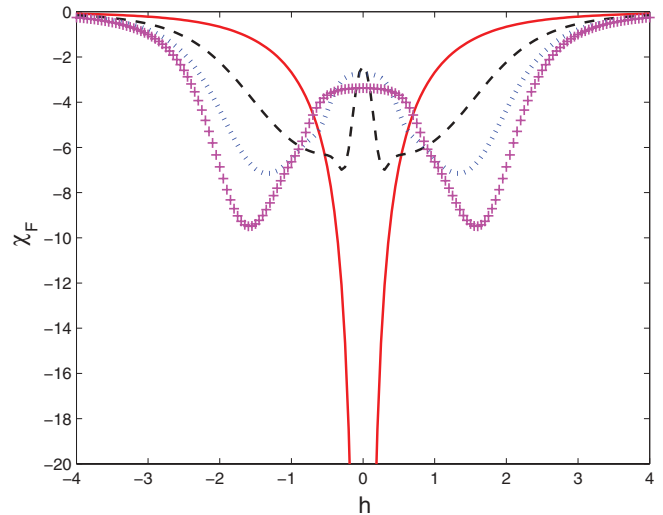


FIG. 1. (Color online) Plot of χ_F versus h for $q = 1, \phi = 0$ (red solid), $q = 2, \phi = \pi/4$ (black dashed), $q = 3, \phi = 0$ (blue dotted), and $q = 4, \phi = \pi/8$ (magenta plus), with $N = 240$ and $\theta = \pi/N$.

We can now use the results obtained in Sec. II to understand various properties of the FS of the model discussed in Sec. III A; we have seen that $\nu = q$ for this model. Further, the parameters in Eq. (4) are given by $g = h$, $u = 2$, and a is given in Eq. (24). If $2\pi/N \ll h^q \ll 1$, the FS should indicate the location of the QCP if $q = 1$, but not if $q \geq 2$.

Figure 1 confirms the above statement for $q = 1, 2, 3$, and 4 , $N = 240$, and $\theta = \pi/N$. For each value of q in that figure, we have chosen ϕ so as to maximize the gap $|\Delta|$ which is proportional to $\cos(q\phi)$ ($\sin(q\phi)$) for q odd (even). At $h = 0$, there is a large peak in $-\chi_F$ for $q = 1$, but not for $q = 2, 3$, and 4 . For $q = 1$, the peak value of $-\chi_F$ is found to be 450 at $h = 0$ which lies far outside the range of Fig. 1; we note that this peak value is consistent with Eq. (9) since $\nu = 1$, $a = 1$, and the Fermi velocity is $u = 2$.

In producing Fig. 1, we have chosen N to be a multiple of 4 and $\theta = \pi/N$ for the following reason. As discussed in Eq. (23), the momentum k introduced in Sec. II is actually the deviation from the momenta $\pm\pi/2$ for the model discussed in Sec. III A. To prevent the expression in Eq. (9) from diverging in our model, we must ensure that $\pm\pi/2 + \theta + 2\pi n/N$ does not vanish for any value of n . This will be true if N is a multiple of 4 and $\theta = \pi/N$. (Alternatively, we could have chosen $N - 2$ to be a multiple of 4 and $\theta = 0$.)

We observe in Fig. 1 that χ_F is not zero at $h = 0$ for $q = 2, 3$, and 4 , in contrast to the result in Eq. (9). We can analytically compute $\chi_F(h = 0)$ by using the following result from first-order perturbation theory. If $H(\lambda) = H_0 + \lambda V$ is a many-body Hamiltonian with eigenvalues $E_\alpha(\lambda)$ and eigenstates $\psi_\alpha(\lambda)$, where $\alpha = 0$ denotes the ground state, then the FS is given by³³

$$\chi_F(\lambda) = -\frac{1}{2} \sum_{\alpha \neq 0} \frac{|\langle \psi_\alpha(\lambda) | V | \psi_0(\lambda) \rangle|^2}{[E_\alpha(\lambda) - E_0(\lambda)]^2}. \quad (31)$$

We now apply this result to our model. At $h = 0$ and $\theta = \pi/N$, the ground state of the total system is one in which the $N/2$ one-particle states with $k = -\pi/2, -\pi/2 + 2\pi/N, \dots, \pi/2 - 2\pi/N$ are filled and the

remaining $N/2$ states are empty. Next, at $h = dh$, the change in the ground state to first order in dh is given by a state in which a fermion has moved from a filled state at k to an empty state at $k - \pi/q$ if k lies in the range $[-\pi/2, -\pi/2 + \pi/q]$, or from k to $k + \pi/q$ if k lies in the range $[\pi/2 - \pi/q, \pi/2]$. Using Eqs. (29) and (30), we find that the FS at $h = 0$ is given by

$$\chi_F(h=0) = - \sum_{k=-\pi/2}^{-\pi/2+\pi/q} \frac{1}{16[\cos(k+\theta) - \cos(k-\pi/q+\theta)]^2}, \quad (32)$$

where k goes in steps of $2\pi/N$, and we have used the fact that the contribution to χ_F from the range $[-\pi/2, -\pi/2 + \pi/q]$ is equal to the contribution from the range $[\pi/2 - \pi/q, \pi/2]$. For large N , we can change the summation in Eq. (32) to an integral $[\sum_k \rightarrow \int dk(N/2\pi)]$ and ignore θ to obtain

$$\chi_F(h=0) = - \frac{N}{32\pi \sin(\pi/q)}. \quad (33)$$

Note that this result does not depend on the phase ϕ in Eq. (14). For $N = 240$ and $q = 2, 3$, and 4 , this gives $\chi_F(h=0) \simeq 2.39, 2.76$, and 3.38 , respectively, which agree well with the values shown in Fig. 1.

Finally we note in Fig. 1 that the FS for $q = 2, 3$, and 4 has a double-peak structure; however, these peaks are unrelated to the QCP at $h = 0$. We notice that as q increases, these peaks move towards $h = \pm 2$. We will see in Sec. IV that in the limit $q \rightarrow \infty$, there are QCPs at $h = \pm 2$ in addition to the QCP at $h = 0$, and the double peaks are an indication of those QCPs.

C. Scaling of fidelity susceptibility with θ

In this section, we will show that by varying θ , we can locate the QCP at $h = 0$ even for $q \geq 2$. Further, the scaling of the FS with respect to θ allows us to find the value of the critical exponent ν . At the end we will also discuss the scaling of the FS with ϕ .

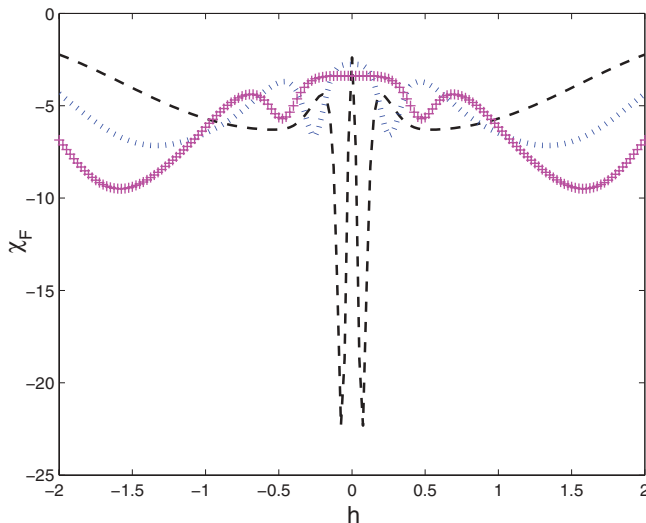


FIG. 2. (Color online) Plot of χ_F versus h for $q = 2, \phi = \pi/4$ (black dashed), $q = 3, \phi = 0$ (blue dotted), and $q = 4, \phi = \pi/8$ (magenta plus), with $N = 240$ and $\theta = 0.001$.

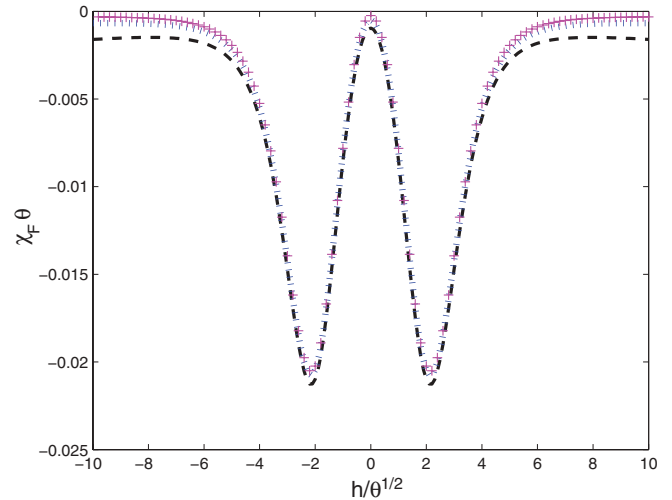


FIG. 3. (Color online) Plot of $\chi_F \theta$ versus $h/\theta^{1/2}$ for $\theta = 0.0004$ (black dashed), $\theta = 0.0002$ (blue dotted), and $\theta = 0.0001$ (magenta plus), with $q = 2$, $N = 240$, and $\phi = \pi/4$.

In Fig. 2, we show the FS for $q = 2, 3$, and 4 , $N = 240$, and $\theta = 0.001$, which is much smaller than the value of $\theta = \pi/N$ chosen in Fig. 1; the values of ϕ chosen for each q are the same as in Fig. 1. We now see that additional double peaks have appeared in the different curves which lie much closer to $h = 0$, with the peak values decreasing and their distances from $h = 0$ increasing as q increases. We will now see that these new peaks are related to the QCP at $h = 0$ and that their peak values and positions scale in accordance with Eq. (8); as $\theta \rightarrow 0$, the locations of the peaks approach the QCP.

In Fig. 3, we show $\chi_F \theta^{2/q}$ versus $h/\theta^{1/q}$ for $q = 2$, $N = 240$, and $\phi = \pi/4$, with $\theta = 0.0004, 0.0002$, and 0.0001 . We see that the three curves fall on top of each other, thus confirming the scaling form given in Eq. (8). In Fig. 4, we show $\chi_F \theta^{2/3}$ versus $h/\theta^{1/3}$ for $q = 3$, $N = 240$, and $\phi = 0$, with $\theta = 0.0001, 0.00003$, and 0.00001 . Once again the curves fall on top of each other.

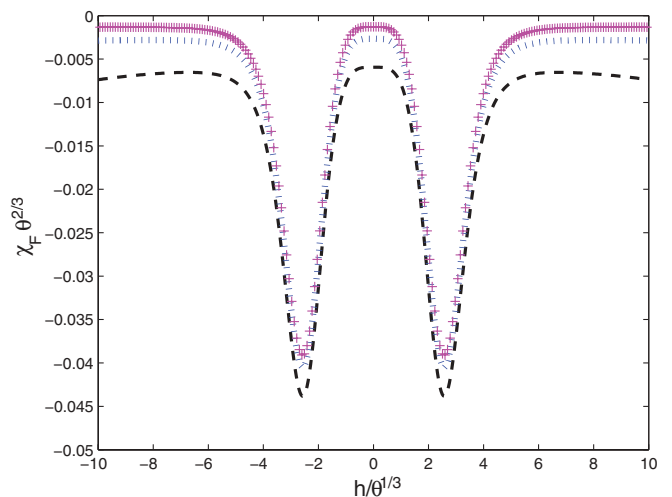


FIG. 4. (Color online) Plot of $\chi_F \theta^{2/3}$ versus $h/\theta^{1/3}$ for $\theta = 0.0001$ (black dashed), $\theta = 0.00003$ (blue dotted), and $\theta = 0.00001$ (magenta plus), with $q = 3$, $N = 240$, and $\phi = 0$.

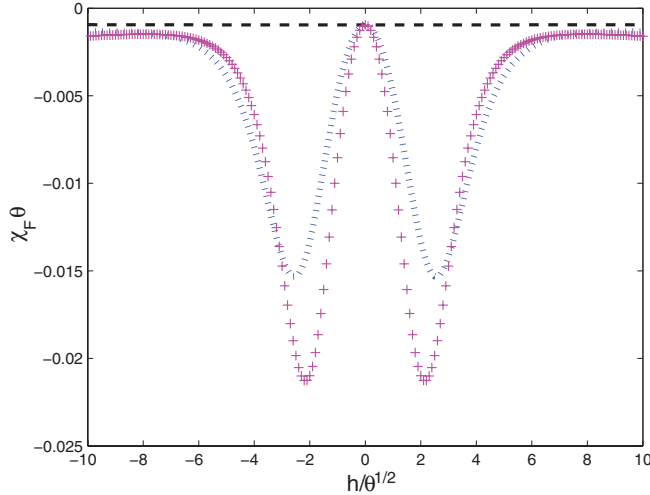


FIG. 5. (Color online) Plot of $\chi_F \theta$ versus $h/\theta^{1/2}$ for $\phi = 0$ (black dashed), $\phi = \pi/8$ (blue dotted), and $\phi = \pi/4$ (magenta plus), with $q = 2$, $N = 240$, and $\theta = 0.0004$.

The values of θ in Figs. 3 and 4 indicate that as q increases from 2 to 3, we have to go to smaller values of θ to see the scaling form. The reason for this is as follows. We saw below Eq. (6) that the peak in the FS occurs at $g/(u\theta)^{1/q} = [(q-1)/(q+1)]^{1/(2q)}$ when $g^q, \theta \ll 2\pi u/N$. In our model, $g = h, u = 2$, and a is given in Eq. (24). Putting these together, we find that the peak occurs at $\theta = (\sqrt{3}/8)h^2$ for $q = 2$ and at $\theta = (\sqrt{2}/24)h^3$ for $q = 3$. We thus see that for a small value of h , θ is smaller for $q = 3$ compared to $q = 2$. For $h = 0.1$, for instance, the peak lies at $\theta \simeq 0.0022$ for $q = 2$ and at $\theta \simeq 0.000059$ for $q = 3$.

It is interesting to consider the dependence of the FS on the phase ϕ . At $h = 0$, we saw that χ_F is given by Eq. (33) and is independent of ϕ . But χ_F does depend on ϕ away from $h = 0$. Figure 5 shows $\chi_F \theta$ versus $h/\theta^{1/2}$ for $q = 2$, $N = 240$, and $\theta = 0.0004$, with $\phi = 0, \pi/8$, and $\pi/4$. The three curves look quite different; in fact, the curve for $\phi = 0$ hardly changes with $h/\theta^{1/2}$ within the range shown in the figure. Note that $\phi = 0$ is the value at which the perturbatively calculated gap Δ given by Eq. (22) vanishes for $q = 2$ and is therefore independent of h within the perturbative range. Hence χ_F is essentially independent of h and is simply given by its value at $h = 0$ if $\phi = 0$. Using Eqs. (6) and (24), we find that for $q = \nu = 2$, $\chi_F \theta$ should be a function of $h|\sin(2\phi)|^{1/2}/\theta^{1/2}$. In Fig. 6, we show $\chi_F \theta$ versus $h|\sin(2\phi)|^{1/2}/\theta^{1/2}$ for $q = 2$, $N = 240$, and $\theta = 0.0001$, with $\phi = \pi/16, \pi/8$, and $\pi/4$. We see that the three curves fall on top of each other thus confirming the presence of the factor of $|\sin(2\phi)|^{1/2}$ in the scaling function.

D. Fidelity susceptibility in another model with $\nu = 2$

It turns out that there is another model in one dimension which has QCPs with $\nu = 2$. This is an anisotropic spin-1/2 XY spin chain in which the strength of a transverse field alternates between $h + \delta$ and $h - \delta$ at odd and even sites.^{53–56}

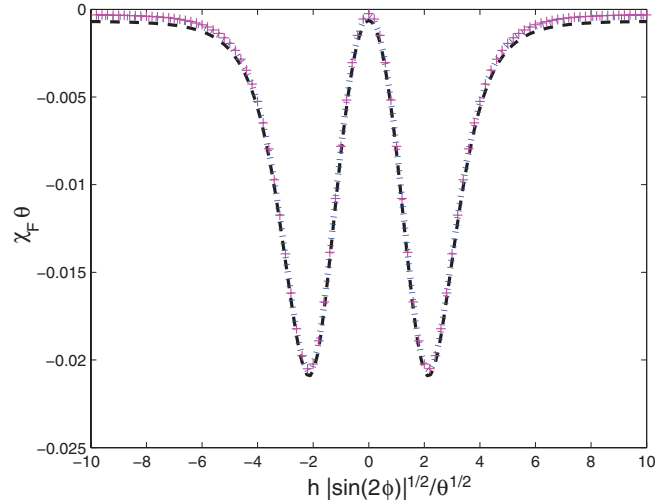


FIG. 6. (Color online) Plot of $\chi_F \theta$ versus $h|\sin(2\phi)|^{1/2}/\theta^{1/2}$ for $\phi = \pi/16$ (black dashed), $\phi = \pi/8$ (blue dotted), and $\phi = \pi/4$ (magenta plus), with $q = 2$, $N = 240$, and $\theta = 0.0001$.

The Hamiltonian of the model is given by

$$H = - \sum_n \left[\frac{(J_x + J_y)}{4} (\sigma_n^x \sigma_{n+1}^x + \sigma_n^y \sigma_{n+1}^y) + \frac{(J_x - J_y)}{4} (\sigma_n^x \sigma_{n+1}^x - \sigma_n^y \sigma_{n+1}^y) + \frac{[h - (-1)^n \delta]}{2} \sigma_n^z \right]. \quad (34)$$

The spectrum of this model can be solved by carrying out the Jordan-Wigner transformation from spin-1/2's to spinless fermions at each site. (The system then decouples into a number of four-dimensional subsystems. We will not present the details here and refer the reader to Refs. 53 and 54.) Defining $J_x + J_y = J$ and $J_x - J_y = \gamma$, we find that the model has four quantum critical lines given by $\delta = \pm\sqrt{h^2 + \gamma^2}$ and $h = \pm\sqrt{\delta^2 + J^2}$. If $\delta = \pm\gamma$ is held fixed, there are QCPs at $h = 0$ which lie on the critical lines $\delta = \pm\sqrt{h^2 + \gamma^2}$. Alternatively, if $h = \pm J$ is held fixed, there are QCPs at $\delta = 0$ which lie on the critical lines $h = \sqrt{\delta^2 + J^2}$. All these QCPs have $z = 1$ and $\nu = 2$.

We have numerically studied the FS of this model after introducing a twist θ in the Jordan-Wigner fermionic Hamiltonian. Holding $J = 2$, $\gamma = 1$, and $h = 2$ fixed, we varied δ to go through the QCP lying at $\delta = 0$. Figure 7 shows the scaling of $\chi_F \theta$ versus $\delta/\theta^{1/2}$ for $N = 240$ and $\theta = 0.0004, 0.0002$, and 0.0001 . The scaling near the QCP at $\delta = 0$ is very similar to what is seen in Fig. 3, just as one would expect from Eq. (8) for a system with $\nu = 2$. This model therefore confirms that the introduction of a twist angle can enable the FS to detect a QCP with $\nu = 2$.

IV. FIDELITY SUSCEPTIBILITY FOR VERY LONG PERIODS

If the quantity π/q in Eq. (14) is replaced by π times an irrational number (which can be approximated by rational numbers with increasingly large denominators), we obtain a quasiperiodic system.^{40–48,50,51} It is known that such a system

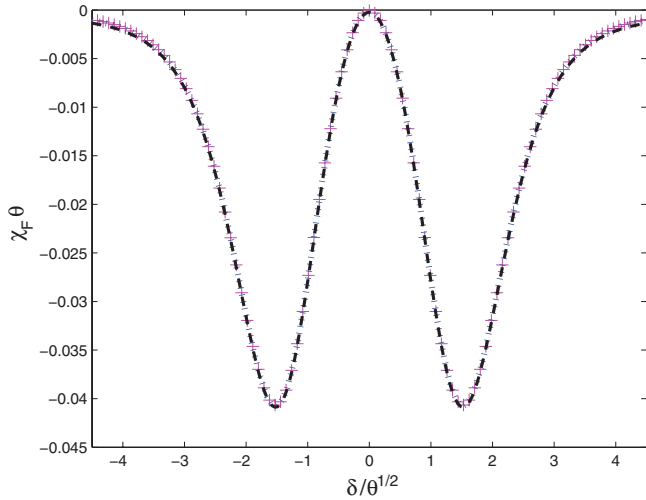


FIG. 7. (Color online) Plot of $\chi_F \theta$ versus $\delta/\theta^{1/2}$ for $\theta = 0.0004$ (black dashed), $\theta = 0.0002$ (blue dotted), and $\theta = 0.0001$ (magenta plus) for the anisotropic spin-1/2 chain with $N = 240$.

has a metal-insulator transition at $h = \pm 2$; the nature of the eigenstate at zero energy changes from extended (metallic) to localized (insulating) on crossing these QCPs.^{45,46,50,51} The FS has been used to detect QCPs in quasiperiodic systems⁵⁷ as well as in disordered systems.⁵⁸

In this section, we will study the FS of the model defined in Eq. (14) as q becomes very large. In that limit, we find numerically that the FS has increasingly large peaks at $h = \pm 2$; we have seen precursors of these peaks in Fig. 1 for $q = 2, 3$, and 4. As far as we know, these QCPs have not been reported earlier. Our results indicate that the metal-insulator transition also seems to occur in our model, although $1/q$ approaches zero rather than an irrational number as $q \rightarrow \infty$.

In Fig. 8, we show the FS for $q = 120, 240$, and 480, with $N = 2q$, $\theta = \pi/N$, and $\phi = \pi/N$ in each case. (Since N must be a multiple of $2q$ and q is quite large, we are only presenting the results for $N = 2q$ here. However, we have checked for $q = 60$ that our results do not change if we take N to be a

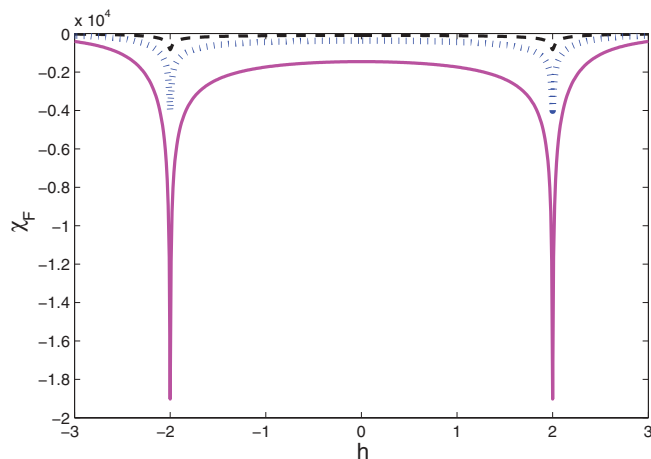


FIG. 8. (Color online) Plot of χ_F versus h for $q = 120$ (black dashed), $q = 240$ (blue dotted), and $q = 480$ (magenta solid), with $N = 2q$, $\theta = \pi/N$, and $\phi = \pi/N$ in each case.

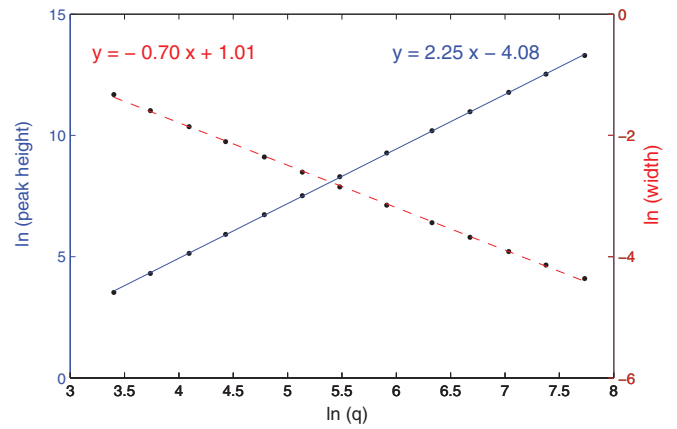


FIG. 9. (Color online) Log-log plot of the peak value (blue solid, y axis on left) and the full width at half maximum (red dashed, y axis on right) versus q for the peak in χ_F at $h = 2$.

higher multiple of $2q$. Further, we have fixed the values of θ and ϕ in terms of N , and will not study here how the FS varies with them.) We observe prominent peaks in the FS at $h = \pm 2$. Figure 9 shows a log-log plot of the peak value and the full width at half maximum versus q for the peak in χ_F at $h = 2$, for a range of values of q from 30 to 2280. We find that the peak value of χ_F scales as $q^{2.25}$ while the full width at half maximum scales as $1/q^{0.70}$. In Fig. 10, we show the scaling near $h = 2$ by plotting $\chi_F/q^{2.25}$ versus $(h - 2)q^{0.70}$ for $q = 120, 240$, and 480; the curves fall on top of each other. Interestingly, we see that the curves are somewhat asymmetric about $h = 2$.

We have also studied the energy gap and the nature of the wave function at zero energy, i.e., the Fermi energy. Upon extrapolating to the thermodynamic limit $N \rightarrow \infty$, we find that the gap is zero even if we are away from $h = \pm 2$; hence these QCPs are different from the ones discussed in the earlier sections where the gap scales as $|h - h_c|^{\nu}$ and is therefore nonzero for $h \neq h_c$ even if $N \rightarrow \infty$ (here h_c denotes the location of the QCP). The QCPs at $h = \pm 2$ are not characterized by the gap going to zero but rather by a change in the nature of the wave function at zero energy.

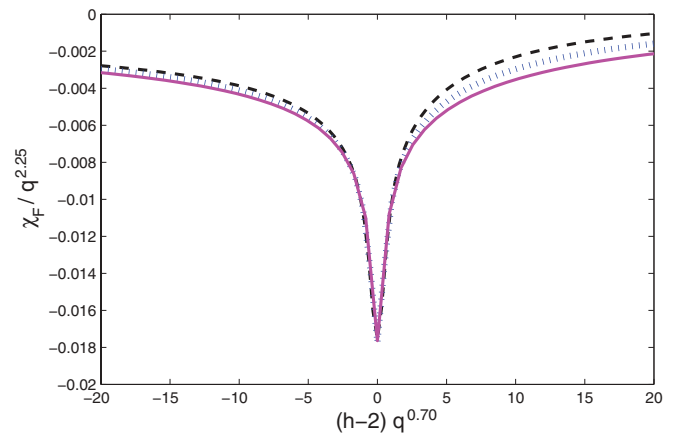


FIG. 10. (Color online) Plot of $\chi_F/q^{2.25}$ versus $(h - 2)q^{0.70}$ for $q = 120$ (black dashed), $q = 240$ (blue dotted), and $q = 480$ (magenta solid), with $N = 2q$, $\theta = \pi/N$, and $\phi = \pi/N$ in each case.

We can understand why the behavior of the system changes at $h = \pm 2$ by using a continuum theory to study the properties of Eq. (14) for a state whose energy lies at zero, i.e., at the Fermi energy. (We will assume here that the limit $N \rightarrow \infty$ has been taken.) A continuum theory is justified if q is very large since the chemical potential then varies on a length scale which is much longer than the lattice spacing a . We can remove the twist angle θ , by performing the phase transformation $c_n \rightarrow e^{-in\theta} c_n$ in Eq. (14), if we are only interested in the behavior of a state in a local region of the system. Setting $J = 1$, the equation of motion following from Eq. (14) is

$$-(c_{n+1} + c_{n-1}) - h \cos\left(\frac{\pi n}{q} + \phi\right) c_n = E c_n \quad (35)$$

for a state with energy E . If c_n varies slowly with n , we can write $2c_n - c_{n+1} - c_{n-1} = -d^2 c(x)/dx^2$, where $x = na$ (we will set $a = 1$). Assuming $h > 0$, we redefine n as $n - n_0$ where n_0 is an integer chosen in such a way that $\pi n_0/q + \phi$ is as close to π as possible; hence $-h \cos(\pi n_0/q + \phi)$ is close to its maximum value of h . (We can choose n_0 in an infinite number of ways; the various choices differ from each other by multiples of $2q$.) We then find that Eq. (35) can be written as a differential equation for $c(x)$,

$$-\frac{d^2 c}{dx^2} + \left[h \cos\left(\frac{\pi x}{q}\right) - 2 \right] c = E c. \quad (36)$$

Equation (36) describes a particle moving in a periodic potential whose maximum value is $h - 2$. The potential has an infinite number of wells, each extending from n_0 to $n_0 + 2q$. If $h < 2$, a state with $E = 0$ lies above the maximum of the potential; in that case the particle can move classically between the different wells, and the wave function will be extended throughout the system. If $h > 2$, a particle with $E = 0$ is classically confined to one particular well of the periodic potential and can only go to other wells by quantum mechanical tunneling. If h is slightly greater than 2, a WKB approximation shows that the tunneling probability between two neighboring wells is proportional to $\exp[-(h - 2)q]$. If $(h - 2)q \gg 1$, the tunneling probability is extremely small, and the wave function is localized within a single well. We thus see that in the limit $q \rightarrow \infty$, $h = 2$ marks a transition between extended and localized wave functions for the state with zero energy.

V. CONCLUSIONS

To summarize, we have shown that in a one-dimensional model which has a QCP with a correlation length exponent $\nu \geq 2$, the introduction of a twist angle θ enables us to use the fidelity susceptibility to determine the location of the QCP. Namely, if the Hamiltonian has a parameter g such that the QCP lies at $g = 0$, the twist allows us to bring the energy of a particular state close to zero. If $\theta \ll 2\pi/N$, the FS scales as $\chi_F \sim \theta^{-2/\nu} f(g/\theta^{1/\nu})$ which makes the QCP clearly visible if χ_F is plotted versus g . A twisted boundary condition therefore provides a powerful tool for locating a QCP which may be difficult to find in any other way. We have argued that this technique may also be useful for finding QCPs in higher dimensional models.

The specific model that we have used to demonstrate this idea is a tight-binding model of spinless fermions with a periodic chemical potential with amplitude h and period $2q$, where q is an integer. We have studied in detail the QCP lying at $h = 0$; at this point, the dynamical critical exponent is given by $z = 1$ while $\nu = q$. This makes this model specially useful for testing what happens for different values of ν . We have shown analytically, using perturbation theory about $h = 0$ and the decoupling of the system into a number of $(2q)$ -dimensional subsystems, that the fidelity susceptibility scales as $\chi_F \sim \theta^{-2/\nu} f(h/\theta^{1/\nu})$ if θ is sufficiently small; we have verified this scaling numerically for small values of q . Although we have not presented the details here, we have confirmed that a similar scaling relation holds in another model which has QCPs with $\nu = 2$. This is an anisotropic spin-1/2 XY chain with transverse fields which has alternating strengths on odd and even sites.

In the last part of the paper, we have considered what happens in our model when q becomes very large. We find that some additional QCPs appear at $h = \pm 2$ in that limit, and the FS is clearly able to detect these QCPs. To the best of our knowledge, these QCPs have not been reported before. We have studied the power laws associated with the peak value and the width of the FS as a function of q ; we find nontrivial powers of 2.25 for the peak value and 0.70 for the width. The energy gap between the ground state and the first excited state is zero in the thermodynamic limit $N \rightarrow \infty$ over a finite range of values of h around these QCPs. This makes it difficult to define the exponent ν at these QCPs (unlike the QCP lying at $h = 0$ where we know that $\nu = q$). Using a continuum theory, we have argued that these QCPs are characterized by a change in the nature of the wave function of a particle at the Fermi energy from extended to localized. In the future it would be interesting to develop a more detailed understanding of these QCPs which may shed some light on the nontrivial power laws that we have found.

The analysis in this paper is expected to be valid for any one-dimensional system which reduces to a theory of noninteracting fermions in the low-energy limit, i.e., close to the Fermi energy. Near a QCP with $z = 1$ and an arbitrary value of the correlation length exponent ν , the modes near the critical momenta ($= \pm\pi/2$ for a half-filled system) can be described by 2×2 Hamiltonians as in Eqs. (4) and (23). From this we can deduce the scaling of the fidelity susceptibility with g and θ . We also argued at the end of Sec. II A that the analysis can be generalized to the case of z not equal to 1 and in Sec. II B to theories of noninteracting fermions in higher dimensions.

The case of interacting systems is more complicated. In one dimension, such systems are typically described by Tomonaga-Luttinger liquid theory which has $z = 1$. In a recent paper,³⁸ some of us studied quenching in an interacting system which is closely related to the model considered in this paper. We argued there that the effect of interactions is to change the value of ν from q to $q/(2 - K)$ where the parameter K depends on the strength of the interactions, provided that K lies in the range $1/2 < K < 2$. (A noninteracting system has $K = 1$, and we then recover the result $\nu = q$.) We expect that a similar result would hold for the fidelity susceptibility of interacting systems; this may be an interesting question for future investigation.

Finally, we note that the twisted boundary condition has been introduced in this paper as a mathematical device to produce a nontrivial scaling of the fidelity susceptibility which can provide information about the value of ν . However, such a boundary condition also admits an interesting physical interpretation. A one-dimensional system with periodic boundary conditions is the same as a circle. Imposing twisted boundary conditions in such a system is equivalent to assigning a charge to the particles and passing a magnetic flux through the middle of the circle so that the Aharonov-Bohm phase (the product

of the charge and the magnetic flux in some appropriate units) is equal to the twist angle $N\theta$. By introducing a twist we are therefore effectively studying the effect of a magnetic flux on the fidelity susceptibility of a system of charged particles moving on a circle.

ACKNOWLEDGMENTS

For financial support, M.T. and A.D. thank CSIR, India, and D.S. thanks DST, India, for Project No. SR/S2/JCB-44/2010.

-
- ¹S. Sachdev, *Quantum Phase Transitions* (Cambridge University Press, Cambridge, 1999).
- ²B. K. Chakrabarti, A. Dutta, and P. Sen, *Quantum Ising Phases and Transitions in Transverse Ising Models*, Lecture Notes in Physics, Vol. m41 (Springer, Heidelberg, 1996).
- ³M. A. Continentino, *Quantum Scaling in Many-Body Systems* (World Scientific, Singapore, 2001).
- ⁴S. L. Sondhi, S. M. Girvin, J. P. Carini, and D. Shahar, *Rev. Mod. Phys.* **69**, 315 (1997).
- ⁵M. Vojta, *Rep. Prog. Phys.* **66**, 2069 (2003).
- ⁶A. Osterloh, L. Amico, G. Falci, and R. Fazio, *Nature (London)* **416**, 608 (2002).
- ⁷T. J. Osborne and M. A. Nielsen, *Phys. Rev. A* **66**, 032110 (2002).
- ⁸L. Campos Venuti, C. Degli Esposti Boschi, and M. Roncaglia, *Phys. Rev. Lett.* **96**, 247206 (2006).
- ⁹G. Vidal, J. I. Latorre, E. Rico, and A. Kitaev, *Phys. Rev. Lett.* **90**, 227902 (2003).
- ¹⁰A. Kitaev and J. Preskill, *Phys. Rev. Lett.* **96**, 110404 (2006).
- ¹¹H. T. Quan, Z. Song, X. F. Liu, P. Zanardi, and C. P. Sun, *Phys. Rev. Lett.* **96**, 140604 (2006).
- ¹²B. Damski, H. T. Quan, and W. H. Zurek, *Phys. Rev. A* **83**, 062104 (2011).
- ¹³H. Ollivier and W. H. Zurek, *Phys. Rev. Lett.* **88**, 017901 (2001).
- ¹⁴R. Dillenschneider, *Phys. Rev. B* **78**, 224413 (2008).
- ¹⁵S. Luo, *Phys. Rev. A* **77**, 042303 (2008).
- ¹⁶M. S. Sarandy, *Phys. Rev. A* **80**, 022108 (2009).
- ¹⁷T. Nag, A. Patra, and A. Dutta, *J. Stat. Mech.* (2011) P08026.
- ¹⁸L. Amico, R. Fazio, A. Osterloh, and V. Vedral, *Rev. Mod. Phys.* **80**, 517 (2008).
- ¹⁹J. I. Latorre and A. Riera, *J. Phys. A* **42**, 504002 (2009).
- ²⁰A. Polkovnikov, K. Sengupta, A. Silva, and M. Vengalattore, *Rev. Mod. Phys.* **83**, 863 (2010).
- ²¹A. Dutta, U. Divakaran, D. Sen, B. K. Chakrabarti, T. F. Rosenbaum, and G. Aeppli, arXiv:1012.0653.
- ²²M. Znidaric and T. Prosen, *J. Phys. A* **36**, 2463 (2003).
- ²³P. Zanardi and N. Paunkovic, *Phys. Rev. E* **74**, 031123 (2006).
- ²⁴L. Campos Venuti and P. Zanardi, *Phys. Rev. Lett.* **99**, 095701 (2007).
- ²⁵P. Zanardi, P. Giorda, and M. Cozzini, *Phys. Rev. Lett.* **99**, 100603 (2007).
- ²⁶P. Buonsante and A. Vezzani, *Phys. Rev. Lett.* **98**, 110601 (2007).
- ²⁷W.-L. You, Y.-W. Li, and S.-J. Gu, *Phys. Rev. E* **76**, 022101 (2007); S. Yang, S.-J. Gu, C.-P. Sun, and H.-Q. Lin, *Phys. Rev. A* **78**, 012304 (2008); S.-J. Gu, H.-M. Kwok, W.-Q. Ning, and H.-Q. Lin, *Phys. Rev. B* **77**, 245109 (2008); S.-J. Gu and H.-Q. Lin, *Europhys. Lett.* **87**, 10003 (2009); S.-J. Gu, *Int. J. Mod. Phys. B* **24**, 4371 (2010).
- ²⁸H.-Q. Zhou, R. Orus, and G. Vidal, *Phys. Rev. Lett.* **100**, 080601 (2008); H.-Q. Zhou, J. H. Zhao, and B. Li, *J. Phys. A* **41**, 492002 (2008); H.-Q. Zhou and J. P. Barjaktarevic, *ibid.* **41**, 412001 (2008); J.-H. Zhao and H.-Q. Zhou, *Phys. Rev. B* **80**, 014403 (2009).
- ²⁹J. Ma, L. Xu, H.-N. Xiong, and X. Wang, *Phys. Rev. E* **78**, 051126 (2008).
- ³⁰E. Eriksson and H. Johannesson, *Phys. Rev. A* **79**, 060301(R) (2009).
- ³¹D. Schwandt, F. Alet, and S. Capponi, *Phys. Rev. Lett.* **103**, 170501 (2009); A. F. Albuquerque, F. Alet, C. Sire, and S. Capponi, *Phys. Rev. B* **81**, 064418 (2010).
- ³²V. Gritsev and A. Polkovnikov, in *Understanding Quantum Phase Transitions*, edited by L. D. Carr (Taylor and Francis, Boca Raton, 2010).
- ³³C. De Grandi, V. Gritsev, and A. Polkovnikov, *Phys. Rev. B* **81**, 012303 (2010); **81**, 224301 (2010).
- ³⁴M. M. Rams and B. Damski, *Phys. Rev. Lett.* **106**, 055701 (2011); *Phys. Rev. A* **84**, 032324 (2011).
- ³⁵J. Sirker, *Phys. Rev. Lett.* **105**, 117203 (2010).
- ³⁶M. Thesberg and E. S. Sørensen, *Phys. Rev. B* **84**, 224435 (2011).
- ³⁷V. Mukherjee, A. Polkovnikov, and A. Dutta, *Phys. Rev. B* **83**, 075118 (2011); V. Mukherjee and A. Dutta, *ibid.* **83**, 214302 (2011); V. Mukherjee, A. Dutta, and D. Sen, *ibid.* **85**, 024301 (2012).
- ³⁸M. Thakurathi, W. DeGottardi, D. Sen, and S. Vishveshwara, *Phys. Rev. B* **85**, 165425 (2012).
- ³⁹W. DeGottardi, D. Sen, and S. Vishveshwara, *New J. Phys.* **13**, 065208 (2011); D. Sen and S. Vishveshwara, *Europhys. Lett.* **91**, 66009 (2010).
- ⁴⁰M. Ya. Azbel, *Zh. Eksp. Teor. Fiz.* **46**, 929 (1964) [*Sov. Phys. JETP* **19**, 634 (1964)]; D. R. Hofstadter, *Phys. Rev. B* **14**, 2239 (1976).
- ⁴¹W. Y. Hsu and L. M. Falicov, *Phys. Rev. B* **13**, 1595 (1976).
- ⁴²S. Aubry and G. André, *Ann. Israel Phys. Soc.* **3**, 133 (1980).
- ⁴³G. M. Obermair and H.-J. Schellnhuber, *Phys. Rev. B* **23**, 5185 (1981); H.-J. Schellnhuber, G. M. Obermair, and A. Rauh, *ibid.* **23**, 5191 (1981).
- ⁴⁴S. Ostlund and R. Pandit, *Phys. Rev. B* **29**, 1394 (1984).
- ⁴⁵J. B. Sokoloff, *Phys. Rep.* **126**, 189 (1985).
- ⁴⁶F. Delyon, *J. Phys. A* **20**, L21 (1987).
- ⁴⁷S. N. Sun and J. P. Ralston, *Phys. Rev. B* **44**, 13603 (1991).
- ⁴⁸P. B. Wiegmann and A. V. Zabrodin, *Phys. Rev. Lett.* **72**, 1890 (1994).
- ⁴⁹D. Sen and S. Lal, *Phys. Rev. B* **61**, 9001 (2000); *Europhys. Lett.* **52**, 337 (2000).

- ⁵⁰C. Aulbach, A. Wobst, G.-L. Ingold, P. Hänggi, and I. Varga, *New J. Phys.* **6**, 70 (2004).
- ⁵¹M. Modugno, *New J. Phys.* **11**, 033023 (2009).
- ⁵²C. Itzykson and J.-B. Zuber, *Quantum Field Theory* (McGraw-Hill, Singapore, 1980).
- ⁵³S. Deng, G. Ortiz, and L. Viola, *Europhys. Lett.* **84**, 67008 (2008).
- ⁵⁴U. Divakaran, A. Dutta, and D. Sen, *Phys. Rev. B* **78**, 144301 (2008).
- ⁵⁵J. H. H. Perk, H. W. Capel, and M. J. Zuilhof, *Physica A* **81**, 319 (1975).
- ⁵⁶K. Okamoto and K. Yasumura, *J. Phys. Soc. Jpn.* **59**, 993 (1990).
- ⁵⁷S. Wen-Guang and T. Pei-Qing, *Chin. Phys. B* **18**, 4707 (2009).
- ⁵⁸J. C. C. Cestari, A. Foerster, and M. A. Gusmao, *Phys. Rev. A* **82**, 063634 (2010).